

Z DECAYS INTO LIGHT GLUINOS: a calculation based on unitarity ¹

Zumin Luo ²

*Enrico Fermi Institute and Department of Physics
University of Chicago, 5640 S. Ellis Avenue, Chicago, IL 60637*

The Z boson can decay to a pair of light gluinos through loop-mediated processes. Based on unitarity of the S -matrix, the imaginary part of the decay amplitude is computed in the presence of a light bottom squark. This imaginary part can provide useful information on the full amplitude. Implications are discussed for a recently proposed light gluino and light bottom squark scenario.

PACS Categories: 11.30.Pb, 12.60.Jv, 13.38.Dg, 14.80.Ly

¹Enrico Fermi Institute preprint EFI 03-02, to appear in Phys. Rev. D.

²zuminluo@midway.uchicago.edu

I Introduction

A relatively light (12–16 GeV) gluino \tilde{g} , along with a lighter (2–5.5 GeV) bottom squark \tilde{b} , has been proposed [1] to explain the excess of the cross section for bottom quark production at hadron colliders. The \tilde{b} squark is assumed to be a mixture of \tilde{b}_L and \tilde{b}_R , the superpartners of b_L and b_R . Other supersymmetric (SUSY) particles, except the other bottom squark \tilde{b}' and one of the top squarks, are assumed to be sufficiently heavy. The masses of \tilde{b}' and the light top squark \tilde{t} are constrained by the electroweak data to be below 180 GeV and 98 GeV, respectively [2]. We follow the convention in Ref. [1] to define

$$\begin{pmatrix} \tilde{b} \\ \tilde{b}' \end{pmatrix} = \begin{pmatrix} \cos \theta_{\tilde{b}} & \sin \theta_{\tilde{b}} \\ -\sin \theta_{\tilde{b}} & \cos \theta_{\tilde{b}} \end{pmatrix} \begin{pmatrix} \tilde{b}_R \\ \tilde{b}_L \end{pmatrix} . \quad (1)$$

The introduction of these new particles gives rise to new interactions in various processes. For example, the total decay width of the Υ is raised since the decay $\Upsilon \rightarrow \tilde{b}\tilde{b}^*$ [3] is now permitted; the decay width of the Z boson is also changed [4, 5]. As a result, the extraction of the strong coupling constant α_s at these two mass scales will be affected. By contributing to the β -function, these SUSY particles slow down the evolution of α_s with energy scale [6]. The situation has recently been studied in detail by Chiang *et al.* [7] and no clear-cut decision can be made in favor of either the Standard Model evolution or the evolution in the light gluino/light bottom squark scenario. The partial decay width $\Gamma(Z \rightarrow \tilde{g}\tilde{g})$ remains a key quantity to be determined. A better evaluation of $\Gamma(Z \rightarrow \tilde{g}\tilde{g})$, among other things, can improve our understanding of the effect of these new particles on the electroweak measurables at the Z pole and hence the determination of $\alpha_s(M_Z)$ in the scenario.

To validate the proposition of these new particles, direct searches for light gluinos and light bottom squarks at e^-e^+ colliders will definitely play a key role. An analysis has been presented recently by Berge and Klasen [8] of gluino pair production at linear e^-e^+ colliders. However, they only considered the mass range $m_{\tilde{g}} \geq 200$ GeV. Production of light gluino pairs was studied by Ref. [9] and its updated version [10]. However, a chirally-mixed *light* bottom squark was not included in either of these calculations. The decay of on-shell Z bosons into gluino pairs was first discussed in Refs. [11, 12], but no chiral mixing between squarks was allowed. Djouadi and Drees [13] took into account chiral mixing and computed an explicit expression for $\Gamma(Z \rightarrow \tilde{g}\tilde{g})$. However, they neglected the gluino mass and required all squark mass eigenstates to be heavier than $M_Z/2$. Production of light gluinos at $p\bar{p}$ colliders was considered by Terekhov and Clavelli [14] but without inclusion of the light bottom squark either. Therefore, an analysis of light gluino production in the presence of a light bottom squark will be very useful for gluino searches.

Although all the previous calculations agree with each other that the branching ratio of $Z \rightarrow \tilde{g}\tilde{g}$ is less than $\mathcal{O}(10^{-3})$, they differ in some important features of the process. At the one-loop level the decay occurs through two types of diagrams; see Fig. 1. In type (a) diagrams the Z couples to a pair of quarks and a squark is exchanged during the process, while in type (b) diagrams the Z couples to two squarks and a quark is exchanged. Refs. [8, 11] disagree with Refs. [10, 13] in the relative

sign between the two types of diagrams. Considering only non-mixed chiral squarks of equal mass, Kane and Rolnick [12] claimed that the amplitude of the process is identically zero when $m_q = m_{\tilde{q}}$ is satisfied for each supersymmetric pair, even if weak isospin is broken so that, for example, $m_t \neq m_b$. However, other references [8, 10, 13] state that for the contribution of quarks and squarks of a given generation to vanish, we must have both mass degeneracy in the quark isospin doublet (e.g., $m_d = m_u$) and mass degeneracy in the squark isospin doublets (e.g., $m_{\tilde{d}} = m_{\tilde{d}'} = m_{\tilde{u}} = m_{\tilde{u}'}$). There are also two contradictory opinions with regard to cancellation of ultraviolet divergences. Refs. [8, 11, 12] asserted that ultraviolet singularities cancel separately for each weak isospin partner, while Djouadi and Drees [13] found that the amplitude is finite only after summing over a complete isodoublet. This discrepancy is essentially related to the relative sign between diagrams (a) and (b) in Fig. 1. The divergent parts of the two diagrams must have opposite signs for them to cancel separately for each isospin partner. There may not be any constraint on the relative sign between (a) and (b) for divergences to cancel within an isodoublet, since the two members in an isodoublet have opposite I_3 (the third component of the weak isospin) and the divergences are generally proportional to I_3 .

A full calculation of $\Gamma(Z \rightarrow \tilde{g}\tilde{g})$ involves evaluation of the Feynman diagrams in Fig. 1, with the cut (s)quark lines connected. To get a meaningful result, one has to deal with difficult one-loop integrals and remove singularities due to on-shell particles. In this paper we try to provide a different approach to solving the above-mentioned discrepancies. Since $2m_b < M_Z$ and $2m_{\tilde{b}} < M_Z$ in the proposed scenario, the decay amplitude has an imaginary part which is finite and can be calculated in an easier way. It is likely that the imaginary part can provide some useful information on the full amplitude. Similar situations arise in the K_S – K_L mass difference and the decay $K_L \rightarrow \mu^+ \mu^-$ [15]. In each case the high-momentum components of the loop diagrams are suppressed (through the presence of the charmed quark [16]), leaving the low-mass on-shell states ($\pi\pi$ or $\gamma\gamma$, respectively) to provide a good estimate of the matrix element. In the light gluino and light bottom squark scenario, the decay width for $Z \rightarrow \tilde{g}\tilde{g}$ usually turns out to be only a few times larger than the contribution from the imaginary part alone.

This paper is organized as follows. Section II establishes the unitarity relation of the \mathcal{M} matrix elements. Amplitudes of the cut diagrams are calculated in Section III and the results are listed in the Appendix. The lower bound based on the imaginary part of the decay amplitude for $Z \rightarrow \tilde{g}\tilde{g}$ is presented in Section IV. Implications of the imaginary part for the full amplitude are discussed in Sections V. Implications for gluino searches and running of α_s are discussed in Sections VI and VII, respectively. Section VIII summarizes.

II Unitarity relation

Let us first review the decays $K_{L,S} \rightarrow l^- l^+$ considered in Ref. [15]. As is the case with $Z \rightarrow \tilde{g}\tilde{g}$, both decays are forbidden at the tree level. However, they can occur through a two-photon ($\gamma\gamma$) intermediate state. Other intermediate states such as $\pi\pi\gamma$

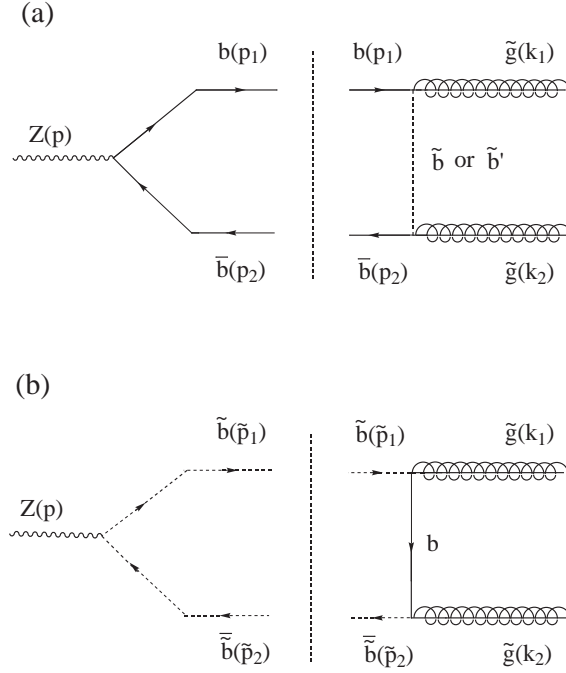


Figure 1: Cut Feynman diagrams for $Z \rightarrow \tilde{g}\tilde{g}$: (a) $Z \rightarrow (\bar{b}b)^* \rightarrow \tilde{g}\tilde{g}$, (b) $Z \rightarrow (\tilde{b}\tilde{b})^* \rightarrow \tilde{g}\tilde{g}$. Similar diagrams with $\tilde{g}(k_1) \leftrightarrow \tilde{g}(k_2)$ are not shown but should be included in the calculation with an overall minus sign.

and 3π are much less important. As a consequence of the unitarity of the S -matrix ($S^\dagger S \equiv (1 + iT)^\dagger (1 + iT) = 1$), the T -matrix element between the initial state $K_{L,S}$ and the final state $l^- l^+$ satisfies the following relation

$$\text{Im} [\langle l^- l^+ | T | K_{L,S} \rangle] = \frac{1}{2} [\langle l^- l^+ | T^\dagger T | K_{L,S} \rangle] \quad , \quad (2)$$

where Im denotes the imaginary part. If we only consider the two-photon intermediate state, then

$$\begin{aligned} \langle l^- l^+ | T^\dagger T | K_{L,S} \rangle &= \sum_{\epsilon, \epsilon'} \int \frac{d^3 k}{(2\pi)^3} \frac{d^3 k'}{(2\pi)^3} \frac{1}{2E} \frac{1}{2E'} \langle l^- l^+ | T^\dagger | \gamma(k, \epsilon) \gamma'(k', \epsilon') \rangle \\ &\quad \times \langle \gamma(k, \epsilon) \gamma'(k', \epsilon') | T | K_{L,S} \rangle \quad , \end{aligned} \quad (3)$$

where $|\gamma(k, \epsilon) \gamma'(k', \epsilon')\rangle$ is a real two-photon state with k and k' , ϵ and ϵ' specifying the 4-momenta and 4-polarizations, respectively. Since the T -matrix elements can be expressed as the invariant \mathcal{M} matrix elements multiplied by 4-momentum-conserving δ -functions, Eqs. (2) and (3) combine to give

$$\begin{aligned} \text{Im} [\mathcal{M}(K_{L,S} \rightarrow l^- l^+)] &= \frac{1}{2} \sum_{\epsilon, \epsilon'} \int \frac{d^3 k}{(2\pi)^3} \frac{d^3 k'}{(2\pi)^3} \frac{1}{2E} \frac{1}{2E'} \langle \gamma(k, \epsilon) \gamma'(k', \epsilon') | \mathcal{M} | K_{L,S} \rangle \\ &\quad \langle \gamma(k, \epsilon) \gamma'(k', \epsilon') | \mathcal{M} | l^- l^+ \rangle^* (2\pi)^4 \delta^{(4)}(p - k_1 - k_2), \end{aligned} \quad (4)$$

times an overall $\delta^{(4)}(p - p_1 - p_2)$, with p , p_1 and p_2 being the 4-momenta of $K_{L,S}$, l^- and l^+ , respectively. It is expected that the real part of the amplitude is roughly of

the same order as the imaginary part, so that the actual decay width will exceed the lower bound based on the imaginary part by only a small factor.

Quite similarly, the imaginary part of the invariant matrix element $\mathcal{M}(Z \rightarrow \tilde{g}\tilde{g})$ at the one-loop level can be written as

$$\text{Im}[\mathcal{M}(Z \rightarrow \tilde{g}\tilde{g})] = \frac{1}{2} \sum_f \int d\Pi_f \mathcal{M}(Z \rightarrow f) \mathcal{M}^*(\tilde{g}\tilde{g} \rightarrow f) (2\pi)^4 \delta^{(4)}(p - \sum_{i=1}^{n_f} p_i), \quad (5)$$

where the sum runs over all possible intermediate on-shell states f and $d\Pi_f = \prod_{i=1}^{n_f} \frac{d^3 p_i}{(2\pi)^3} \frac{1}{2E_i}$ with n_f being the numbers of particles in state f and p_i being the 3-momenta of the particles. Since \tilde{b} is the lightest supersymmetric particle in the scenario and all other supersymmetric particles (except \tilde{g}) are expected to be heavier than $M_Z/2$, we only need to consider the cases where f is $b\bar{b}$ and $\tilde{b}\tilde{b}^*$. The integral over the phase space Π_f can be simplified to the integral over the solid angle Ω . In the case where the intermediate state is two particles with equal masses, we have $\int d\Pi_f (2\pi)^4 \delta^{(4)}(p - \sum_{i=1}^{n_f} p_i) = \frac{v}{32\pi^2} \int d\Omega$, where v is the velocity of the on-shell intermediate particles.

III Amplitudes of the cut diagrams

We adopt the spinor convention of Peskin and Schroeder [17], in which the metric tensor $g_{\mu\nu} = \text{Diagonal}(1, -1, -1, -1)$ and

$$\gamma^0 = \begin{pmatrix} 0 & 1 \\ 1 & 0 \end{pmatrix}, \quad \gamma^5 = \begin{pmatrix} -1 & 0 \\ 0 & 1 \end{pmatrix} \quad \text{and} \quad \gamma^i = \begin{pmatrix} 0 & \sigma^i \\ -\sigma^i & 0 \end{pmatrix}, \quad i = 1, 2, 3, \quad (6)$$

where σ^i are the Pauli matrices. The uncrossed cut Feynman diagrams that contribute to the imaginary part of the full amplitude are shown in Fig. 1. The crossed diagrams with $\tilde{g}(k_1) \leftrightarrow \tilde{g}(k_2)$ are not shown but should also be included in the calculation. In the center-of-mass frame of the Z boson, the 4-momenta of the final gluinos are $k_1 = (E, \mathbf{k})$ and $k_2 = (E, -\mathbf{k})$, where $E = M_Z/2$ and $\mathbf{k} = (0, 0, |\mathbf{k}|)$. Suppose \mathbf{k} is along the z -axis and the polarizations of the Z are quantized along this axis, i.e., $\epsilon^\mu = (0, 1, \pm i, 0)/\sqrt{2}$ or $(0, 0, 0, 1)$, corresponding to helicities $\lambda = \pm 1$ or 0 respectively. The 4-momenta of the intermediate bottom quarks are $p_1 = (E, \mathbf{p})$ and $p_2 = (E, -\mathbf{p})$, with $\mathbf{p} = |\mathbf{p}|(\sin \theta \cos \phi, \sin \theta \sin \phi, \cos \theta)$. The 4-momenta of the intermediate bottom squarks are $\tilde{p}_1 = (E, \tilde{\mathbf{p}})$ and $\tilde{p}_2 = (E, -\tilde{\mathbf{p}})$, with $\tilde{\mathbf{p}} = |\tilde{\mathbf{p}}|(\sin \theta \cos \phi, \sin \theta \sin \phi, \cos \theta)$. The Feynman rules for the Majorana fields are given in a representation independent way in [18].

The \mathcal{M} matrix element for $Z \rightarrow b\bar{b}$ is

$$\mathcal{M}(Z \rightarrow b\bar{b}) = -\frac{g_W}{2 \cos \theta_W} \bar{u}(p_1) \not{\epsilon}(p) (g_L^b P_L + g_R^b P_R) v(p_2) \delta^{ij}, \quad (7)$$

where $\not{\epsilon} \equiv \epsilon \cdot \gamma$, $g_L^b = g_V^b + g_A^b = \frac{2}{3} \sin^2 \theta_W - 1$, $g_R^b = g_V^b - g_A^b = \frac{2}{3} \sin^2 \theta_W$, $P_L = \frac{1-\gamma^5}{2}$, $P_R = \frac{1+\gamma^5}{2}$, δ^{ij} is a Kronecker delta in the quark color indices and $p = p_1 + p_2$ is the

4-momentum of the Z . The Dirac spinors $u(p_1)$ and $v(p_2)$ can be written as

$$\begin{aligned} u^\uparrow(p_1) &= \begin{pmatrix} \sqrt{E - |\mathbf{p}|} \xi^\uparrow \\ \sqrt{E + |\mathbf{p}|} \xi^\uparrow \end{pmatrix} & u^\downarrow(p_1) &= \begin{pmatrix} \sqrt{E + |\mathbf{p}|} \xi^\downarrow \\ \sqrt{E - |\mathbf{p}|} \xi^\downarrow \end{pmatrix} \\ v^\uparrow(p_2) &= \begin{pmatrix} \sqrt{E - |\mathbf{p}|} \eta^\uparrow \\ -\sqrt{E + |\mathbf{p}|} \eta^\uparrow \end{pmatrix} & v^\downarrow(p_2) &= \begin{pmatrix} \sqrt{E + |\mathbf{p}|} \eta^\downarrow \\ -\sqrt{E - |\mathbf{p}|} \eta^\downarrow \end{pmatrix} \end{aligned} \quad , \quad (8)$$

where the arrows \uparrow and \downarrow denote spin up and spin down along \mathbf{p} , respectively;

$$\begin{aligned} \xi^\uparrow &= \begin{pmatrix} \cos \frac{\theta}{2} \\ e^{i\phi} \sin \frac{\theta}{2} \end{pmatrix} & \xi^\downarrow &= \begin{pmatrix} -e^{-i\phi} \sin \frac{\theta}{2} \\ \cos \frac{\theta}{2} \end{pmatrix} \\ \eta^\uparrow &= \begin{pmatrix} -\sin \frac{\theta}{2} \\ e^{i\phi} \cos \frac{\theta}{2} \end{pmatrix} & \eta^\downarrow &= \begin{pmatrix} e^{-i\phi} \cos \frac{\theta}{2} \\ \sin \frac{\theta}{2} \end{pmatrix} \end{aligned} \quad .$$

We then have

$$\begin{aligned} \mathcal{M}(Z \rightarrow b^\uparrow \bar{b}^\uparrow) &= (0, i \sin \phi + \cos \phi \cos \theta, -i \cos \phi + \sin \phi \cos \theta, -\sin \theta) \cdot \epsilon(p) \\ &\quad \times \frac{g_W}{2 \cos \theta_W} [(E - |\mathbf{p}|) g_L^b + (E + |\mathbf{p}|) g_R^b] \delta^{ij} \\ \mathcal{M}(Z \rightarrow b^\downarrow \bar{b}^\downarrow) &= (0, -i \sin \phi + \cos \phi \cos \theta, i \cos \phi + \sin \phi \cos \theta, -\sin \theta) \cdot \epsilon(p) \\ &\quad \times \frac{g_W}{2 \cos \theta_W} [(E + |\mathbf{p}|) g_L^b + (E - |\mathbf{p}|) g_R^b] \delta^{ij} \\ \mathcal{M}(Z \rightarrow b^\uparrow \bar{b}^\downarrow) &= \frac{g_W m_b}{2 \cos \theta_W} e^{-i\phi} [g_L^b (-1, \sin \theta \cos \phi, \sin \theta \sin \phi, \cos \theta) \\ &\quad + g_R^b (1, \sin \theta \cos \phi, \sin \theta \sin \phi, \cos \theta)] \cdot \epsilon(p) \delta^{ij} \\ \mathcal{M}(Z \rightarrow b^\downarrow \bar{b}^\uparrow) &= -\frac{g_W m_b}{2 \cos \theta_W} e^{i\phi} [g_L^b (1, \sin \theta \cos \phi, \sin \theta \sin \phi, \cos \theta) \\ &\quad + g_R^b (-1, \sin \theta \cos \phi, \sin \theta \sin \phi, \cos \theta)] \cdot \epsilon(p) \delta^{ij} \end{aligned}$$

For $\sin^2 \theta_W = 0.2311$ and without top quark corrections, the partial decay width for Z to decay into massless $b\bar{b}$ is then $\frac{G_F M_Z^3}{4\sqrt{2}\pi} [(g_L^b)^2 + (g_R^b)^2] = 368 \text{ MeV}$.

Now we consider $b\bar{b} \rightarrow \tilde{g}\tilde{g}$ via exchange of a \tilde{b} or \tilde{b}' , the matrix element for which is denoted $\mathcal{M}(b\bar{b} \rightarrow \tilde{g}\tilde{g})$ or $\mathcal{M}'(b\bar{b} \rightarrow \tilde{g}\tilde{g})$, respectively. We have $\mathcal{M}(b\bar{b} \rightarrow \tilde{g}\tilde{g}) = \mathcal{M}^{(1)}(b\bar{b} \rightarrow \tilde{g}\tilde{g}) + \mathcal{M}^{(2)}(b\bar{b} \rightarrow \tilde{g}\tilde{g})$, with

$$\begin{aligned} \mathcal{M}^{(1)}(b\bar{b} \rightarrow \tilde{g}\tilde{g}) &= -2g_s^2 \frac{(t^b t^a)_{ji}}{(p_1 - k_1)^2 - m_{\tilde{b}}^2} \bar{u}(k_1) (P_L \sin \theta_{\tilde{b}} - P_R \cos \theta_{\tilde{b}}) u(p_1) \\ &\quad \bar{v}(p_2) (P_R \sin \theta_{\tilde{b}} - P_L \cos \theta_{\tilde{b}}) \tilde{v}(k_2), \end{aligned} \quad (9)$$

$$\begin{aligned} \mathcal{M}^{(2)}(b\bar{b} \rightarrow \tilde{g}\tilde{g}) &= -2g_s^2 \frac{(t^a t^b)_{ji}}{(p_1 - k_2)^2 - m_{\tilde{b}}^2} \tilde{v}^T(k_2) C^{-1} (P_L \sin \theta_{\tilde{b}} - P_R \cos \theta_{\tilde{b}}) u(p_1) \\ &\quad \bar{v}(p_2) (P_R \sin \theta_{\tilde{b}} - P_L \cos \theta_{\tilde{b}}) C \tilde{u}^T(k_1), \end{aligned} \quad (10)$$

where the superscript (1) denotes the uncrossed diagram and (2) the crossed diagram; a, b and i, j are the color indices of the gluinos and the quarks, respectively; t^a are

the fundamental representation matrices of $SU(3)$; $C = i\gamma^0\gamma^2$ is the charge conjugate matrix. It can be easily verified that $u(p, s) = C\bar{v}^T(p, s)$ and $v(p, s) = C\bar{u}^T(p, s)$, where T means “transpose”. The Majorana spinors $\tilde{u}(k_1)$ and $\tilde{v}(k_2)$ also satisfy these relations [18]. Thus we can immediately write

$$\begin{aligned}\tilde{u}^\uparrow(k_1) &= \begin{pmatrix} \sqrt{E - |\mathbf{k}|}\zeta_+ \\ \sqrt{E + |\mathbf{k}|}\zeta_+ \end{pmatrix} & \tilde{u}^\downarrow(k_1) &= \begin{pmatrix} \sqrt{E + |\mathbf{k}|}\zeta_- \\ \sqrt{E - |\mathbf{k}|}\zeta_- \end{pmatrix} \\ \tilde{u}^\uparrow(k_2) &= \begin{pmatrix} \sqrt{E + |\mathbf{k}|}\zeta_+ \\ \sqrt{E - |\mathbf{k}|}\zeta_+ \end{pmatrix} & \tilde{u}^\downarrow(k_2) &= \begin{pmatrix} -\sqrt{E - |\mathbf{k}|}\zeta_- \\ -\sqrt{E + |\mathbf{k}|}\zeta_- \end{pmatrix} \\ \tilde{v}^\uparrow(k_1) &= \begin{pmatrix} \sqrt{E + |\mathbf{k}|}\zeta_- \\ -\sqrt{E - |\mathbf{k}|}\zeta_- \end{pmatrix} & \tilde{v}^\downarrow(k_1) &= \begin{pmatrix} -\sqrt{E - |\mathbf{k}|}\zeta_+ \\ \sqrt{E + |\mathbf{k}|}\zeta_+ \end{pmatrix} \\ \tilde{v}^\uparrow(k_2) &= \begin{pmatrix} \sqrt{E - |\mathbf{k}|}\zeta_- \\ -\sqrt{E + |\mathbf{k}|}\zeta_- \end{pmatrix} & \tilde{v}^\downarrow(k_2) &= \begin{pmatrix} \sqrt{E + |\mathbf{k}|}\zeta_+ \\ -\sqrt{E - |\mathbf{k}|}\zeta_+ \end{pmatrix} \end{aligned}, \quad (11)$$

with $\zeta_+ = \begin{pmatrix} 1 \\ 0 \end{pmatrix}$ and $\zeta_- = \begin{pmatrix} 0 \\ 1 \end{pmatrix}$. Here the arrows \uparrow and \downarrow denote spin up and spin down along \mathbf{k} (i.e., the z -axis), respectively. Since $\tilde{v}^T(k_2)C^{-1} = -\tilde{u}(k_2)$ and $C\tilde{u}^T(k_1) = \tilde{v}(k_1)$, Eq. (10) can alternatively be obtained from Eq. (9) by interchanging k_1 and k_2 and adding an overall minus sign. The helicities of the final gluinos are determined by λ , the initial helicity of the Z . For $\lambda = 1$, both gluinos have spin up in the z -direction, while for $\lambda = -1$, both have spin down in the z -direction. For $\lambda = 0$, one of them has spin up and the other has spin down in the z -direction. One expects $|\text{Im}\mathcal{M}(Z^\downarrow \rightarrow \tilde{g}^\downarrow\tilde{g}^\downarrow)| = |\text{Im}\mathcal{M}(Z^\uparrow \rightarrow \tilde{g}^\uparrow\tilde{g}^\uparrow)|$, because the two processes are related by mirror symmetry. One also expects $\text{Im}\mathcal{M}(Z^{(0)} \rightarrow \tilde{g}^\uparrow\tilde{g}^\downarrow) = 0$, because these final gluinos have the same helicities and should therefore be excluded by the Pauli principle. The matrix element $\mathcal{M}'(b\bar{b} \rightarrow \tilde{g}\tilde{g})$ can be obtained from $\mathcal{M}(b\bar{b} \rightarrow \tilde{g}\tilde{g})$ by replacing $m_{\tilde{b}}$, $\sin\theta_{\tilde{b}}$ and $\cos\theta_{\tilde{b}}$ with $m_{\tilde{b}'}$, $\cos\theta_{\tilde{b}}$ and $-\sin\theta_{\tilde{b}}$, respectively.

Now consider the diagram in Fig. 1 (b) and a similar diagram with $\tilde{g}(k_1) \leftrightarrow \tilde{g}(k_2)$, where the intermediate state is a pair of scalar quarks (\tilde{b} and $\tilde{\bar{b}}$). The tree-level $Z\tilde{b}\tilde{\bar{b}}$ coupling is proportional to $g_L^b \sin^2\theta_{\tilde{b}} + g_R^b \cos^2\theta_{\tilde{b}}$, so a mixing angle of $\theta_{\tilde{b}} = \arcsin\sqrt{2\sin^2\theta_W/3} \simeq 23^\circ$ or 157° will make it vanish. A weak $Z\tilde{b}\tilde{\bar{b}}$ coupling is assumed [1] to satisfy the tight constraints imposed by precision measurements at the Z peak. Consequently the contribution of the $\tilde{b}\tilde{\bar{b}}$ intermediate state to $\text{Im}\mathcal{M}(Z \rightarrow \tilde{g}\tilde{g})$ should also be small. However, to see how the two types of diagrams shown in Fig. 1 interfere with each other, we take $\theta_{\tilde{b}}$ to be a free parameter. For the first part of the cut diagram [Fig. 1 (b)], we have

$$\mathcal{M}(Z \rightarrow \tilde{b}\tilde{\bar{b}}) = -\frac{g_W}{2\cos\theta_W} \left[g_L^b \sin^2\theta_{\tilde{b}} + g_R^b \cos^2\theta_{\tilde{b}} \right] (\tilde{p}_1 - \tilde{p}_2)^\mu \epsilon_\mu(p) \delta^{ij}, \quad (12)$$

where i and j are the squark color indices. The sign discrepancy mentioned in the Introduction can be traced to the relative sign between Eqs. (7) and (12) [8]. The

current sign in Eq. (12) is consistent with the Feynman rules in Ref. [18]. We will argue in favor of this sign from another point of view in Section V. For the other part of the diagram,

$$\begin{aligned}\mathcal{M}^{(1)}(\tilde{b}\tilde{b} \rightarrow \tilde{g}\tilde{g}) &= 2g_s^2 \frac{(t^b t^a)_{ji}}{(\tilde{p}_1 - k_1)^2 - m_b^2} \tilde{v}^T(k_2) C^{-1} [P_L \sin \theta_{\tilde{b}} - P_R \cos \theta_{\tilde{b}}] \\ &\quad (\not{\tilde{p}}_1 - \not{k}_1 + m_b) [P_R \sin \theta_{\tilde{b}} - P_L \cos \theta_{\tilde{b}}] C \tilde{u}^T(k_1)\end{aligned}\quad (13)$$

$$\begin{aligned}\mathcal{M}^{(2)}(\tilde{b}\tilde{b} \rightarrow \tilde{g}\tilde{g}) &= 2g_s^2 \frac{(t^a t^b)_{ji}}{(\tilde{p}_1 - k_2)^2 - m_b^2} \tilde{u}(k_1) [P_L \sin \theta_{\tilde{b}} - P_R \cos \theta_{\tilde{b}}] \\ &\quad (\not{\tilde{p}}_1 - \not{k}_2 + m_b) [P_R \sin \theta_{\tilde{b}} - P_L \cos \theta_{\tilde{b}}] \tilde{v}(k_2),\end{aligned}\quad (14)$$

where (1) denotes the uncrossed diagram and (2) the crossed diagram. The relevant matrix elements for $\lambda = 1$ are presented in the Appendix.

IV Lower bound on $\Gamma(Z \rightarrow \tilde{g}\tilde{g})$

Now we are ready to put things together and obtain a lower bound on $\Gamma(Z \rightarrow \tilde{g}\tilde{g})$. First we consider an extreme case with $m_b = m_{\tilde{b}} = m_{\tilde{g}} = 0$ and $m_{\tilde{b}'} = \infty$. In this limit, the product $\mathcal{M}(Z \rightarrow f)\mathcal{M}(f \rightarrow \tilde{g}\tilde{g})$ has an angular dependence of either $(1 + \cos \theta)$ or $(1 - \cos \theta)$. However, the $\cos \theta$ term does not contribute to the imaginary part of the full amplitude, because integrating it over the solid angle Ω gives zero. Note that $\text{tr}(t^a t^b) = \text{tr}(t^b t^a) = \delta^{ab}/2$. The only nonvanishing amplitudes are

$$\begin{aligned}\mathcal{M}(Z^\uparrow \rightarrow b\bar{b}) * \mathcal{M}(b\bar{b} \rightarrow \tilde{g}^\uparrow \tilde{g}^\uparrow) &= \delta^{ab} r_W (g_A^b - g_V^b \cos 2\theta_{\tilde{b}}) \\ \mathcal{M}(Z^\downarrow \rightarrow b\bar{b}) * \mathcal{M}(b\bar{b} \rightarrow \tilde{g}^\downarrow \tilde{g}^\downarrow) &= -\delta^{ab} r_W (g_A^b - g_V^b \cos 2\theta_{\tilde{b}}) \\ \mathcal{M}(Z^\uparrow \rightarrow \tilde{b}\tilde{b}) * \mathcal{M}(\tilde{b}\tilde{b} \rightarrow \tilde{g}^\uparrow \tilde{g}^\uparrow) &= \delta^{ab} r_W (g_V^b - g_A^b \cos 2\theta_{\tilde{b}}) \cos 2\theta_{\tilde{b}} \\ \mathcal{M}(Z^\downarrow \rightarrow \tilde{b}\tilde{b}) * \mathcal{M}(\tilde{b}\tilde{b} \rightarrow \tilde{g}^\downarrow \tilde{g}^\downarrow) &= -\delta^{ab} r_W (g_V^b - g_A^b \cos 2\theta_{\tilde{b}}) \cos 2\theta_{\tilde{b}}\end{aligned}\quad ,$$

where the asterisks imply that we have integrated over the phase spaces and summed over all intermediate helicity states, $r_W = \frac{M_Z g_W g_s^2}{2\sqrt{2} \cos \theta_W}$. From the above equations we can see that the imaginary parts of diagrams (a) and (b) in Fig. 1 interfere destructively if \tilde{b} is more left-handed ($45^\circ < \theta_{\tilde{b}} < 135^\circ$) or dominantly right-handed ($\theta_{\tilde{b}} < 23^\circ$ or $\theta_{\tilde{b}} > 157^\circ$); the contribution of diagram (b) remains negligible in the neighborhood of the decoupling angle (23° or 157°). The imaginary parts of the amplitudes are

$$\begin{aligned}\text{Im}\mathcal{M}(Z^\uparrow \rightarrow \tilde{g}^\uparrow \tilde{g}^\uparrow) &= -\text{Im}\mathcal{M}(Z^\downarrow \rightarrow \tilde{g}^\downarrow \tilde{g}^\downarrow) \\ &= \delta^{ab} r_W (g_L^b - g_R^b) \sin^2 \theta_{\tilde{b}} \cos^2 \theta_{\tilde{b}} / (8\pi)\end{aligned}\quad (15)$$

The relation (15) also holds when all the particles have a finite mass. The lower bound on $\Gamma(Z \rightarrow \tilde{g}\tilde{g})$ in the limit $m_b = m_{\tilde{b}} = m_{\tilde{g}} = 0$ and $m_{\tilde{b}'} = \infty$ can be expressed as a ratio

$$\begin{aligned}\frac{\Gamma(Z \rightarrow \tilde{g}\tilde{g})}{\Gamma(Z \rightarrow b\bar{b})} &\geq \frac{1}{2} \frac{[\text{Im}\mathcal{M}(Z^\uparrow \rightarrow \tilde{g}^\uparrow \tilde{g}^\uparrow)]^2 + [\text{Im}\mathcal{M}(Z^\downarrow \rightarrow \tilde{g}^\downarrow \tilde{g}^\downarrow)]^2}{[\text{Im}\mathcal{M}(Z^\uparrow \rightarrow b^\uparrow \bar{b}^\uparrow)]^2 + [\text{Im}\mathcal{M}(Z^\downarrow \rightarrow b^\downarrow \bar{b}^\downarrow)]^2} \\ &= \frac{\alpha_s^2}{6} \frac{(g_L^b - g_R^b)^2 \sin^4 \theta_{\tilde{b}} \cos^4 \theta_{\tilde{b}}}{(g_L^b)^2 + (g_R^b)^2}\end{aligned}\quad (16)$$

The factor of $1/2$ comes in because the final gluinos are identical. Taking $\Gamma(Z \rightarrow b\bar{b}) = 368$ MeV, we plot the lower bound on the decay width $\Gamma(Z \rightarrow \tilde{g}\tilde{g})$ as a function of the bottom squark mixing angle $\theta_{\tilde{b}}$ in Fig. 2 (dotted curve). When all the masses are finite, we can no longer ignore the $\cos\theta$ terms, because the denominators of the propagators are no longer of the form $\sim (1 \pm \cos\theta)$, which previously cancelled with the same factors in the numerators of the amplitudes and gave only linear terms in $\cos\theta$. However, it is still not hard to perform the integration over the angles. Define

$$\begin{aligned} I_{\pm}(x, y, z) &= \frac{1}{2} \int_0^{\pi} \frac{(1 \pm \cos\theta)^2}{x^2 + y^2 + z^2 + 2xy \cos\theta} \sin\theta d\theta \\ I_0(x, y, z) &= \int_0^{\pi} \frac{\sin^2\theta}{x^2 + y^2 + z^2 + 2xy \cos\theta} \sin\theta d\theta \quad , \end{aligned} \quad (17)$$

and let $c_{\pm} = I_{\pm}(v_b, v_{\tilde{g}}, r_{\tilde{b}})$, $c'_{\pm} = I_{\pm}(v_b, v_{\tilde{g}}, r_{\tilde{b}'})$, $c_0 = I_0(v_b, v_{\tilde{g}}, r_{\tilde{b}})$, $c'_0 = I_0(v_b, v_{\tilde{g}}, r_{\tilde{b}'})$, $\tilde{c}_0 = I_0(v_{\tilde{b}}, v_{\tilde{g}}, r_b)$, where $r_i = 2m_i/M_Z$ ($i = b, \tilde{b}, \tilde{b}', \tilde{g}$), $v_i = \sqrt{1 - r_i^2}$ is the “velocity” of an on-shell particle i ($i = b, \tilde{b}, \tilde{g}$). The lower bound can then be written as

$$\Gamma(Z \rightarrow \tilde{g}\tilde{g}) \geq \frac{G_F M_Z^3 \alpha_s^2}{96\sqrt{2}\pi} (\mathcal{A}_1 v_b + \mathcal{A}'_1 v_b + \mathcal{A}_2 v_{\tilde{b}})^2 v_{\tilde{g}} \quad , \quad (18)$$

where, up to a common factor of proportionality, $\mathcal{A}_1 v_b$ and $\mathcal{A}'_1 v_b$ are the imaginary parts of the amplitudes for $Z \rightarrow (b\bar{b})^* \rightarrow \tilde{g}\tilde{g}$ via exchange of a \tilde{b} and \tilde{b}' , respectively; $\mathcal{A}_2 v_{\tilde{b}}$ is the imaginary part of the amplitude for $Z \rightarrow (\tilde{b}\tilde{b})^* \rightarrow \tilde{g}\tilde{g}$. We have

$$\begin{aligned} \mathcal{A}_1 &= c_1(g_A^b - g_V^b \cos 2\theta_{\tilde{b}}) - g_A^b(c_2 + c_3 \sin 2\theta_{\tilde{b}}) \\ \mathcal{A}'_1 &= c'_1(g_A^b + g_V^b \cos 2\theta_{\tilde{b}}) - g_A^b(c'_2 - c'_3 \sin 2\theta_{\tilde{b}}) \\ \mathcal{A}_2 &= \tilde{c}_0 v_{\tilde{b}}^2 v_{\tilde{g}} (g_V^b - g_A^b \cos 2\theta_{\tilde{b}}) \cos 2\theta_{\tilde{b}} \quad , \end{aligned}$$

where $c_1 = c_-(v_{\tilde{g}} - v_b) + c_+(v_{\tilde{g}} + v_b) + c_0 r_b^2 v_{\tilde{g}}$, $c_2 = (c_- + c_+ + c_0) r_b^2 v_{\tilde{g}}$, $c_3 = (c_+ - c_-) v_b r_b r_{\tilde{g}}$; c'_1 , c'_2 and c'_3 are defined similarly, with c_{\pm} and c_0 all primed. All these quantities only depend on the masses. As m_b , $m_{\tilde{b}}$ and $m_{\tilde{g}}$ go to zero and $m_{\tilde{b}'}$ goes to infinity, $c_1 \rightarrow 1$, $\tilde{c}_0 v_{\tilde{b}}^2 v_{\tilde{g}} \rightarrow 1$, $c_2 \rightarrow 0$, $c_3 \rightarrow 0$, $c'_1 \rightarrow 0$, $c'_2 \rightarrow 0$ and $c'_3 \rightarrow 0$. Eq. (16) is thus recovered. As far as the imaginary part of the amplitude is concerned, Eq. (18) agrees with Ref. [13] in the limit $m_{\tilde{g}} = 0$ except for the mentioned sign discrepancy. Compared to Ref. [13], this unitarity calculation not only takes into account a nonzero gluino mass but also is much simpler. Firstly, there are no singularities to remove. Secondly, one only has to evaluate a few elementary integrals in Eq. (17) instead of the much more difficult one-loop two- and three-point functions.

The lower bound is plotted in Fig. 2 (solid curve) as a function of $\theta_{\tilde{b}}$ for a specific set of values for the masses: $m_b = 4.1$ GeV, $m_{\tilde{b}} = 4.5$ GeV, $m_{\tilde{b}'} = 170$ GeV, $m_{\tilde{g}} = 15$ GeV. The small peak around 90° disappears if the gluino has a small mass (e.g., $m_{\tilde{g}} \leq 7$ GeV) such that the sign of the sum $\mathcal{A}_1 v_b + \mathcal{A}'_1 v_b + \mathcal{A}_2 v_{\tilde{b}}$ does not change over $0^\circ \leq \theta_{\tilde{b}} \leq 180^\circ$. If \tilde{g} were massless, the lower bound as a function of $0^\circ \leq \theta_{\tilde{b}} \leq 180^\circ$ would have two identical peaks (see the dashed curve in Fig. 3). Due to destructive interference between diagrams (a) and (b) for $45^\circ < \theta_{\tilde{b}} < 135^\circ$, $\theta_{\tilde{b}} < 23^\circ$ and $\theta_{\tilde{b}} > 157^\circ$, the lower bound is smaller than the contribution from the $b\bar{b}$ intermediate state alone (Fig. 2, dashed curve) in these ranges.

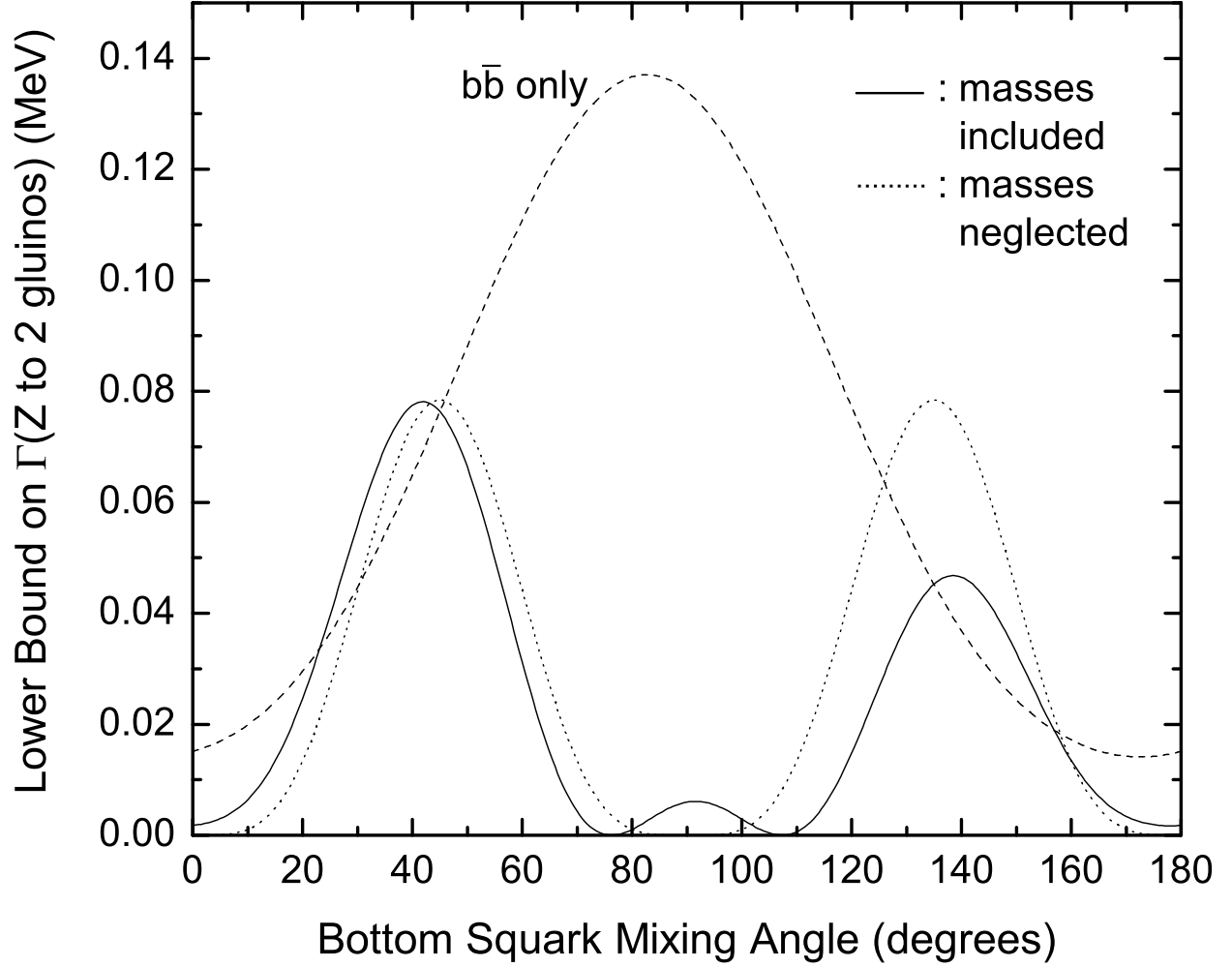


Figure 2: Lower bound on $\Gamma(Z \rightarrow \tilde{g}\tilde{g})$ as a function of the bottom squark mixing angle $\theta_{\tilde{b}}$. Solid curve: $m_b = 4.1$ GeV, $m_{\tilde{b}} = 4.5$ GeV, $m_{\tilde{g}} = 15$ GeV, $m_{\tilde{b}'} = 170$ GeV; dashed curve: only the contribution from the $b\bar{b}$ intermediate state is included with the same set of masses; dotted curve: $m_b = m_{\tilde{b}} = m_{\tilde{g}} = 0$ and $m_{\tilde{b}'} = \infty$.

V Implications for the full decay width $\Gamma(Z \rightarrow \tilde{g}\tilde{g})$

Let us first examine under what conditions the decay amplitude vanishes. We will see that Kane and Rolnick's claim [12] contradicts our unitarity calculation. Under their assumption, $m_{\tilde{q}} = m_{\tilde{q}'} = m_q$ and $\theta_{\tilde{q}} = 0$, so that $c_i = c'_i$ ($i = 1, 2, 3$) and $\tilde{c}_0 = \tilde{c}'_0 \equiv I_0(v_{\tilde{b}'}, v_{\tilde{g}}, r_b) = \pm c_0$. We regard the relative sign (\pm) between diagrams (a) and (b) as undecided and only consider the contribution of the third generation, i.e., $q = t, b$. Define $\mathcal{A}'_2 \equiv -\tilde{c}'_0 v_{\tilde{b}'}^2 v_{\tilde{g}} (g_V^b + g_A^b \cos 2\theta_{\tilde{b}}) \cos 2\theta_{\tilde{b}}$. Then the imaginary part of the amplitude is proportional to $\mathcal{A}_1 + \mathcal{A}'_1 + \mathcal{A}_2 + \mathcal{A}'_2 = 2[(c_+ + c_- \mp c_0)v_{\tilde{b}}^2 v_{\tilde{g}} + (c_+ - c_-)v_b]g_A^b$, which is nonzero for either sign. Therefore, the amplitude does *not* vanish under Kane and Rolnick's conditions. For the imaginary part to be zero, we must have $m_t = m_b$ and $m_{\tilde{t}} = m_{\tilde{t}'} = m_{\tilde{b}} = m_{\tilde{b}'}$ and similar mass degeneracies in the other two generations. (Of course, the imaginary part of the amplitude automatically vanishes if all quark and squark mass eigenstates are heavier than $M_Z/2$.) This is true whether the relative sign between diagrams (a) and (b) is $+$ or $-$ and is consistent with Refs. [8, 10, 13].

Let us now investigate whether the imaginary part of the amplitude computed in the previous section can give us some hint how loop divergences cancel and reasonably small decay widths for $Z \rightarrow \tilde{g}\tilde{g}$ can be obtained. Without actually calculating the full amplitude, we should be able to recover part of it from the imaginary part. For simplicity we take $m_{\tilde{g}} = 0$ and consider only diagram (b) in Fig. 1. The imaginary part of the amplitude for this diagram is proportional to $\mathcal{A}_2 v_{\tilde{b}} = \tilde{c}_0 v_{\tilde{b}}^3 (g_V^b - g_A^b \cos 2\theta_{\tilde{b}}) \cos 2\theta_{\tilde{b}}$. We have

$$\frac{\pi}{2} \tilde{c}_0 v_{\tilde{b}}^3 = \left[\frac{1}{2} - \frac{m_{\tilde{b}}^2 - m_b^2}{s} \right] v_{\tilde{b}} \pi + \left[m_{\tilde{b}}^2 + \frac{(m_{\tilde{b}}^2 - m_b^2)^2}{s} \right] \frac{\pi}{s} \log \frac{(m_{\tilde{b}}^2 - m_b^2)/s - (1 - v_{\tilde{b}})/2}{(m_{\tilde{b}}^2 - m_b^2)/s - (1 + v_{\tilde{b}})/2},$$

where $s = M_Z^2$. For $m_{\tilde{b}} < M_Z/2$, one can check that

$$\begin{aligned} \text{Im} B_0(s, m_{\tilde{b}}, m_{\tilde{b}}) &= v_{\tilde{b}} \pi \\ \text{Im} C_0(s, m_{\tilde{b}}, m_{\tilde{b}}, m_b) &= \frac{\pi}{s} \log \frac{(m_{\tilde{b}}^2 - m_b^2)/s - (1 - v_{\tilde{b}})/2}{(m_{\tilde{b}}^2 - m_b^2)/s - (1 + v_{\tilde{b}})/2}, \end{aligned}$$

where B_0 and C_0 are the scalar one-loop two- and three-point functions [13, 19, 20, 21], respectively. If we define

$$\begin{aligned} A(m_1, m_2, m_3) &= \left[\frac{1}{2} - \frac{(m_1^2 - m_3^2) + (m_2^2 - m_3^2)}{2s} \right] B_0(s, m_1, m_2) \\ &\quad + \left[m_3^2 + \frac{(m_1^2 - m_3^2)(m_2^2 - m_3^2)}{s} \right] C_0(s, m_1, m_2, m_3), \end{aligned}$$

then by analyticity and symmetry, the following terms should be part of the full amplitude contributed by type (b) diagrams in Fig. 1,

$$\begin{aligned} &A(m_{\tilde{b}}, m_{\tilde{b}}, m_b)(g_V^b - g_A^b \cos 2\theta_{\tilde{b}}) \cos 2\theta_{\tilde{b}} - A(m_{\tilde{b}'}, m_{\tilde{b}'}, m_b)(g_V^b + g_A^b \cos 2\theta_{\tilde{b}}) \cos 2\theta_{\tilde{b}} \\ &- A(m_{\tilde{b}}, m_{\tilde{b}'}, m_b) 2g_A^b \sin^2 2\theta_{\tilde{b}} + A(m_{\tilde{t}}, m_{\tilde{t}}, m_t)(g_V^t - g_A^t \cos 2\theta_{\tilde{t}}) \cos 2\theta_{\tilde{t}} \\ &- A(m_{\tilde{t}'}, m_{\tilde{t}'}, m_t)(g_V^t + g_A^t \cos 2\theta_{\tilde{t}}) \cos 2\theta_{\tilde{t}} - A(m_{\tilde{t}}, m_{\tilde{t}'}, m_t) 2g_A^t \sin^2 2\theta_{\tilde{t}}. \end{aligned} \quad (19)$$

Here the $\sin^2 2\theta_{\tilde{q}}$ terms can be obtained by repeating the unitarity calculation with $f = \tilde{b}\tilde{b}'$. Alternatively, they can easily be guessed if we note that the above terms should sum up to zero for $m_t = m_b$ and $m_{\tilde{t}} = m_{\tilde{t}'} = m_{\tilde{b}} = m_{\tilde{b}'}$. Those terms in Eq. (19) are expected to be the only ones relevant to our argument [13].

The top and bottom squark masses and mixing angles are determined by the following mass matrices [13]

$$M_t^2 = \begin{pmatrix} m_{\tilde{t}_L}^2 + m_t^2 + g_L^t s \cos 2\beta/2 & -m_t(A_t + \mu \cot \beta) \\ -m_t(A_t + \mu \cot \beta) & m_{\tilde{t}_R}^2 + m_t^2 - g_R^t s \cos 2\beta/2 \end{pmatrix} \quad (20)$$

$$M_b^2 = \begin{pmatrix} m_{\tilde{b}_L}^2 + m_b^2 + g_L^b s \cos 2\beta/2 & -m_b(A_b + \mu \tan \beta) \\ -m_b(A_b + \mu \tan \beta) & m_{\tilde{b}_R}^2 + m_b^2 - g_R^b s \cos 2\beta/2 \end{pmatrix}, \quad (21)$$

where $m_{\tilde{t}_L}^2, m_{\tilde{t}_R}^2, m_{\tilde{b}_L}^2, m_{\tilde{b}_R}^2$ are soft SUSY breaking masses; $\tan \beta$ is the ratio of the vacuum expectation values of the two neutral Higgs fields in the MSSM; A_t, A_b denote the trilinear Higgs-stop, -sbottom couplings, respectively; and μ is the Higgsino mass parameter. $SU(2)$ gauge invariance leads to $m_{\tilde{t}_L}^2 = m_{\tilde{b}_L}^2$. It is reasonable to assume that we should get a sensible decay width $\Gamma(Z \rightarrow \tilde{g}\tilde{g})$ for each specific set of parameters. In particular, we can choose very large values for $m_{\tilde{t}}, m_{\tilde{t}'}, m_{\tilde{b}}, m_{\tilde{b}'}$ and should find a tiny $\Gamma(Z \rightarrow \tilde{g}\tilde{g})$ for some mixing angles $\theta_{\tilde{t}}$ and $\theta_{\tilde{b}}$. For simplicity we assume $A_t + \mu \cot \beta = A_b + \mu \tan \beta = 0$ so that there is no L - R squark mixing, and

$$\begin{aligned} m_{\tilde{t}_L}^2 + g_L^t s \cos 2\beta/2 &= m_{\tilde{t}_R}^2 - g_R^t s \cos 2\beta/2 \\ m_{\tilde{t}_L}^2 + g_L^b s \cos 2\beta/2 &= m_{\tilde{b}_R}^2 - g_R^b s \cos 2\beta/2 \end{aligned}$$

so that $m_{\tilde{t}} = m_{\tilde{t}'}, m_{\tilde{b}} = m_{\tilde{b}'}$. The mass difference between the top and bottom squarks is then

$$m_{\tilde{t}} - m_{\tilde{b}} = \sqrt{m_{\tilde{t}_L}^2 + m_t^2 + g_L^t s \cos 2\beta/2} - \sqrt{m_{\tilde{t}_L}^2 + m_b^2 + g_L^b s \cos 2\beta/2} \approx \frac{\delta m^2}{m_{\tilde{t}_L}},$$

with $\delta m^2 \equiv [2(m_{\tilde{t}}^2 - m_{\tilde{b}}^2) + (g_L^t - g_L^b)s \cos 2\beta]/4$. The sum in Eq. (19) becomes simply

$$A(m_{\tilde{b}}, m_{\tilde{b}}, m_b) - A(m_{\tilde{t}}, m_{\tilde{t}}, m_t) \equiv \delta A. \quad (22)$$

In the heavy squark limit,

$$\begin{aligned} B_0(s, m_{\tilde{q}}, m_{\tilde{q}}) &= \Delta + \log \frac{m_{\tilde{q}}^2}{\nu^2} \\ C_0(s, m_{\tilde{q}}, m_{\tilde{q}}, m_q) &= -\frac{1}{m_{\tilde{q}}^2 - m_q^2} + \frac{m_q^2}{(m_{\tilde{q}}^2 - m_q^2)^2} \log \frac{m_{\tilde{q}}^2}{m_q^2}, \end{aligned}$$

where Δ denotes the ultraviolet divergent part of B_0 and ν is the renormalization scale. We can see that the B_0 and C_0 terms in $A(m_{\tilde{q}}, m_{\tilde{q}}, m_q)$ vary as $-(m_{\tilde{q}}^2 - m_q^2)[\log m_{\tilde{q}}^2/\nu^2]/s$ and $-(m_{\tilde{q}}^2 - m_q^2)/s$, respectively. So the leading term in δA comes from B_0 and varies as

$$[(m_{\tilde{t}}^2 - m_t^2) \log m_{\tilde{t}}^2 - (m_{\tilde{b}}^2 - m_b^2) \log m_{\tilde{b}}^2]/s \sim [(g_L^t - g_L^b) \cos 2\beta \log m_{\tilde{t}_L}^2]/2.$$

Thus the sum in Eq. (19) is logarithmically divergent as $m_{\tilde{t}_L}$ goes to infinity. Therefore, we cannot get reasonable decay widths if this divergence is supposed to cancel within an isodoublet. So we do not agree with Djouadi and Drees' claim [13] that one can get meaningful results by summing over a complete isodoublet. The only other way out is for the divergence to cancel for each weak isospin partner. Note that the ultraviolet divergent parts of the B_0 terms in Eq. (19) not only can cancel within an isodoublet, but also can cancel for each weak isospin partner. Indeed, if the relative sign between diagrams (a) and (b) in Ref. [13] is reversed, one finds that both ultraviolet divergences and the divergences in the heavy squark limit (as discussed above) cancel separately for the top and bottom sectors. To understand how the latter divergences cancel, repeat the same reasoning as that leading to Eq. (19) for type (a) diagrams in Fig. 1 and observe that those diagrams should contribute the following terms,

$$\pm \left[C(m_b, m_b, m_{\tilde{b}})(g_A^b - g_V^b \cos 2\theta_{\tilde{b}}) + C(m_b, m_b, m_{\tilde{b}'}) (g_A^b + g_V^b \cos 2\theta_{\tilde{b}}) \right. \\ \left. C(m_t, m_t, m_{\tilde{t}})(g_A^t - g_V^t \cos 2\theta_{\tilde{t}}) + C(m_t, m_t, m_{\tilde{t}'}) (g_A^t + g_V^t \cos 2\theta_{\tilde{t}}) \right] \quad , \quad (23)$$

where again we keep an undecided relative sign and

$$C(m_1, m_1, m_2) \equiv \left[m_1^2 + \frac{(m_2^2 - m_1^2)^2}{s} \right] C_0(s, m_1, m_1, m_2) \quad .$$

For $m_{\tilde{t}} = m_{\tilde{t}'}$ and $m_{\tilde{b}} = m_{\tilde{b}'}$, Eq. (23) becomes

$$\pm [C(m_t, m_t, m_{\tilde{t}}) - C(m_b, m_b, m_{\tilde{b}})] \equiv \pm \delta C \quad . \quad (24)$$

One can check that when $m_{\tilde{q}}$ becomes large,

$$\text{Re}C_0(s, m_q, m_q, m_{\tilde{q}}) \sim -\frac{1}{m_{\tilde{q}}^2 - m_q^2} \log \frac{m_{\tilde{q}}^2}{s} \quad .$$

Thus the leading term in $\text{Re}\delta C$ is exactly the same as the leading term in δA . The second-to-leading and higher order terms turn out to be finite after summing over $q = t, b$ (for either relative sign) *or* over diagrams (a) and (b) (for only one of the signs). If we have chosen a correct relative sign, the divergences in type (b) diagrams should cancel exactly with those in type (a) diagrams *separately* for $q = t, b$. Otherwise the divergences will add up and the total amplitude will be logarithmically divergent as the squark masses go to infinity. We find that the sign in the current note rather than that in Ref. [13] is favored.

Our numerical analysis not only verifies the above argument but also shows that it works even if arbitrary L - R squark mixing is allowed and the above constraints on the parameters are relaxed. Using the same formula in Ref. [13] but *with* the sign flipped³, we find that for $m_{\tilde{g}} \simeq 0$, $m_{\tilde{b}} \leq \mathcal{O}(30)$ GeV, $m_{\tilde{b}'} = \mathcal{O}(150)$ GeV, $m_{\tilde{t}} = \mathcal{O}(90)$ GeV, $m_{\tilde{t}'} = \mathcal{O}(300)$ GeV, $\Gamma(Z \rightarrow \tilde{g}\tilde{g})$ is typically of order 0.1 MeV if b is not dominantly

³The formula fails to produce sensible decay widths in the heavy squark limit if the sign is not reversed, as argued in the text.

left-handed and only of order 0.01 MeV or less if \tilde{b} is dominantly left-handed, i.e., $\theta_{\tilde{b}} \approx 90^\circ$; and that the top squark mixing angle $\theta_{\tilde{t}}$ has little effect on the decay width. If all squark masses are greater than $M_Z/2$, we confirm the statement in Ref. [13] that $\Gamma(Z \rightarrow \tilde{g}\tilde{g})$ depends weakly on the details of L - R squark mixing and find that it is of order 0.1 MeV for a wide range of MSSM parameters. Thus inclusion of a dominantly left-handed light \tilde{b} would reduce the decay width $\Gamma(Z \rightarrow \tilde{g}\tilde{g})$, as is the case for the unitarity lower bound plotted in Fig. 2. A relatively heavy or not very left-handed \tilde{b} will not change the decay width by much. In Fig. 3 we plot the full decay widths as well as the corresponding unitarity lower bounds for $m_{\tilde{g}} = 0$ and two sets of squark masses. When all the squark mass eigenstates are heavier than $M_Z/2$, the full width is about an order of magnitude larger than the lower bound. When one of the bottom squarks is light ($\leq \mathcal{O}(30)$ GeV), the shape of the full width as a function of $\theta_{\tilde{b}}$ is similar to the lower bound and generally only a few times higher than the latter. Although an expression for $\Gamma(Z \rightarrow \tilde{g}\tilde{g})$ is not available when $m_{\tilde{g}} \neq 0$, we expect the shape of $\Gamma(Z \rightarrow \tilde{g}\tilde{g})$ to be also similar to and only a few times higher than the unitarity lower bound plotted in Fig. 2 (solid curve) if the gluino has a mass around 15 GeV and the light bottom squark has a mass around 4.5 GeV. So $\Gamma(Z \rightarrow \tilde{g}\tilde{g})$ should be of order 0.1 MeV in the light gluino and light bottom squark scenario.

VI Implications for gluino searches in Z decays

Aside from $Z \rightarrow \tilde{g}\tilde{g}$, there exist three other gluino-producing Z decays, $Z \rightarrow b\tilde{b}\tilde{g}$, $Z \rightarrow \bar{b}\tilde{b}\tilde{g}$ and $Z \rightarrow q\bar{q}\tilde{g}\tilde{g}$. The first two processes are $\sim \alpha\alpha_s$ at the tree level and have a combined decay width of 1.9 – 5.9 MeV depending on the sign of $\sin 2\theta_{\tilde{b}}$ [22]. The third process is $\sim \alpha\alpha_s^2$ and its decay width is calculated in a model-independent way to be 0.75 – 0.21 MeV for $m_{\tilde{g}} = 12$ –16 GeV [23]. A recent analysis [24] shows that $\Gamma(Z \rightarrow b\tilde{b}\tilde{g}\tilde{g})$ can be enhanced by 10% – 60% due to additional “sbottom splitting” diagrams. This will raise $\Gamma(Z \rightarrow q\bar{q}\tilde{g}\tilde{g})$ by $\mathcal{O}(0.01)$ MeV. The new SUSY particles do not always contribute positively to the Z width, however. Cao *et al.* [5] and S.w. Baek [25] showed that the decay width $\Gamma(Z \rightarrow b\bar{b})$ can be reduced by 2 – 8 MeV. By fine-tuning the parameters in the light gluino and light bottom squark scenario, all the electroweak measurables (Γ_Z , $\Gamma_{\text{had}}(Z)$, R_b , R_c) at the Z pole can be still within the 1σ bounds of the experimental values. Thus, existence of the new particles can only be verified through direct searches for gluinos or bottom squarks. The light bottom squark is assumed to be long-lived at the collider scale or to decay promptly to light hadrons in this scenario. In either case, it forms a hadronic jet within the detector due to its color charge. \tilde{g} decays exclusively to $b\bar{b}$ or $\bar{b}b$ and becomes two hadronic jets. The smallness of $\Gamma(Z \rightarrow \tilde{g}\tilde{g})$ implies the insignificance of $Z \rightarrow \tilde{g}\tilde{g}$ in gluino searches. Searches for signals of $Z \rightarrow b\bar{b}\tilde{g} + \bar{b}b\tilde{g}$ and $Z \rightarrow q\bar{q}\tilde{g}\tilde{g}$ will be expected to play a pivotal role.

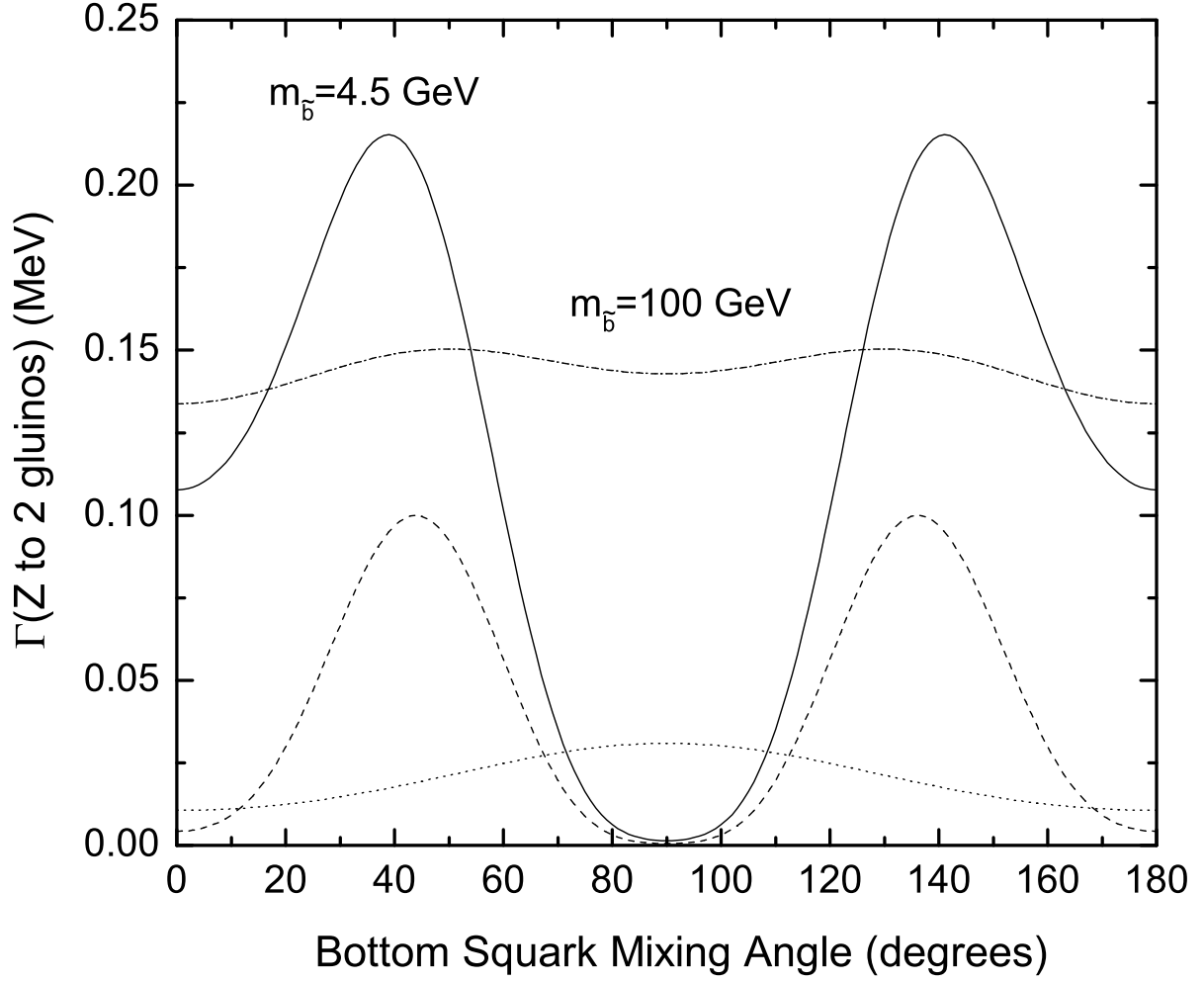


Figure 3: $\Gamma(Z \rightarrow \tilde{g}\tilde{g})$ as a function of the bottom squark mixing angle $\theta_{\tilde{b}}$. We take $\theta_{\tilde{t}} = 50^\circ$, $m_b = 4.1 \text{ GeV}$, $m_{\tilde{b}'} = 170 \text{ GeV}$, $m_t = 174 \text{ GeV}$, $m_{\tilde{t}} = 95 \text{ GeV}$, $m_{\tilde{t}'} = 300 \text{ GeV}$, $m_{\tilde{g}} = 0$. Solid (full width) and dashed (unitarity lower bound) curves: $m_{\tilde{b}} = 4.5 \text{ GeV}$; dash-dotted (full width) and dotted curves (unitarity lower bound): $m_{\tilde{b}} = 100 \text{ GeV}$.

VII Implications for running of α_s

Both the light gluino \tilde{g} and the light bottom squark \tilde{b} can change the β -function that governs the energy-scale dependence (“running”) of the strong coupling constant α_s . At the two-loop level, $\alpha_s(M_Z)$ can be raised by 0.014 ± 0.001 [7] with respect to its standard model value if extrapolated from the mass scale m_b . A natural question arises: are values of $\alpha_s(M_Z)$ determined from measurements at different energy scales still in accordance in the presence of \tilde{g} and \tilde{b} ? To answer this question, the effects of the new SUSY particles on measurements at different scales must be analyzed. For example, the hadronic width of the Z is changed in two ways: 1) the interference of the standard model diagrams and the diagrams with the SUSY particles in loops will reduce the partial width of $Z \rightarrow b\bar{b}$; 2) the existence of the new decay channels $Z \rightarrow \tilde{b}\bar{\tilde{b}}$, $Z \rightarrow \tilde{g}\bar{\tilde{g}}$, $Z \rightarrow \tilde{b}\bar{\tilde{g}}/\bar{\tilde{b}}\tilde{g}$ and $Z \rightarrow q\bar{q}\tilde{g}\bar{\tilde{g}}$ will raise the hadronic width. The bottom squark mixing angle $\theta_{\tilde{b}}$ is chosen to be near 23° or 157° so that $\Gamma(Z \rightarrow \tilde{b}\bar{\tilde{b}})$ is suppressed ⁴. $\Gamma(Z \rightarrow \tilde{g}\bar{\tilde{g}})$ is only of order 0.1 MeV at either of these angles. Thus these two channels combined will change the predicted hadronic width of the Z by a very small amount compared to the decrease in $\Gamma(Z \rightarrow b\bar{b})$ and the increase in $\Gamma_{\text{had}}(Z)$ due to $Z \rightarrow \tilde{b}\bar{\tilde{g}}/\bar{\tilde{b}}\tilde{g}$ and $Z \rightarrow q\bar{q}\tilde{g}\bar{\tilde{g}}$. A better determination of $\Gamma(Z \rightarrow b\bar{b})$, $\Gamma(Z \rightarrow \tilde{b}\bar{\tilde{g}}/\bar{\tilde{b}}\tilde{g})$ and $\Gamma(Z \rightarrow q\bar{q}\tilde{g}\bar{\tilde{g}})$, or a more precise measurement of R_b (which will constrain the value of $\Gamma(Z \rightarrow b\bar{b})$ more tightly), is needed for a clear-cut decision in favor of either the Standard Model or the light gluino and light bottom squark scenario.

VIII Summary

We have calculated the imaginary part of the decay amplitude for $Z \rightarrow \tilde{g}\bar{\tilde{g}}$ and used it to analyze the full amplitude and solve some discrepancies in the literature. We have confirmed the argument that the decay width vanishes if both quarks and squarks of a given generation are degenerate in mass (the quarks and squarks in that generation do not need to have equal mass). We have found that both divergences in the heavy squark limit and ultraviolet divergences cancel for each weak isospin partner, as previously claimed by Refs. [11, 12]. We also favor the relative sign of Refs. [8, 11] between diagrams (a) and (b) in Fig. 1. Borrowing the formula for $\Gamma(Z \rightarrow \tilde{g}\bar{\tilde{g}})$ from Ref. [13] but with their relative sign between diagrams (a) and (b) flipped to be consistent with our calculation, we find that the decay width is of order 0.1 MeV in the proposed light gluino and light bottom squark scenario. Compared with other decay processes like $Z \rightarrow \tilde{b}\bar{\tilde{g}}/\bar{\tilde{b}}\tilde{g}$ and $Z \rightarrow q\bar{q}\tilde{g}\bar{\tilde{g}}$, $Z \rightarrow \tilde{g}\bar{\tilde{g}}$ will only play a moderate role in searches for gluinos and analysis of effects of the SUSY scenario on $\alpha_s(M_Z)$.

⁴ $\Gamma(Z \rightarrow \tilde{b}\bar{\tilde{b}})$ will be greater than 15 MeV if $40^\circ \leq \theta_{\tilde{b}} \leq 140^\circ$.

Acknowledgements

I would like to thank Jonathan L. Rosner, Cheng-Wei Chiang, Abdelhak Djouadi and Manuel Drees for very useful discussions and suggestions. This work was supported in part by the U. S. Department of Energy through Grant Nos. DE-FG02-90ER-40560.

Appendix: relevant M-matrix elements

We define

$$\begin{aligned}
A^{(1)} &= -2g_s^2 \frac{(t^b t^a)_{ji}}{(p_1 - k_1)^2 - m_b^2} \\
A^{(2)} &= -2g_s^2 \frac{(t^a t^b)_{ji}}{(p_1 - k_2)^2 - m_b^2} \\
\tilde{A}^{(1)} &= -2g_s^2 \frac{(t^b t^a)_{ji}}{(\tilde{p}_1 - k_1)^2 - m_b^2} \\
\tilde{A}^{(2)} &= -2g_s^2 \frac{(t^a t^b)_{ji}}{(\tilde{p}_1 - k_2)^2 - m_b^2} \\
B_{\pm\pm} &= \sqrt{(E \pm |\mathbf{k}|)(E \pm |\mathbf{p}|)} \\
\tilde{B}_{\pm\pm} &= \sqrt{(E \pm |\mathbf{k}|)(E \pm |\mathbf{k}|)} \\
S_{\tilde{b}} &= \sin \theta_{\tilde{b}} \\
C_{\tilde{b}} &= \cos \theta_{\tilde{b}}
\end{aligned}$$

\mathcal{M} matrix elements for $Z^\uparrow \rightarrow b\bar{b} \rightarrow \tilde{g}^\uparrow \tilde{g}^\uparrow$:

$$\begin{aligned}
\mathcal{M}(Z^\uparrow \rightarrow b^\uparrow \bar{b}^\uparrow) &= -\frac{g_W}{\sqrt{2} \cos \theta_W} e^{i\phi} \left[(E - |\mathbf{p}|) g_L^b + (E + |\mathbf{p}|) g_R^b \right] \frac{1 + \cos \theta}{2} \delta^{ij} \\
\mathcal{M}^{(1)}(b^\uparrow \bar{b}^\uparrow \rightarrow \tilde{g}^\uparrow \tilde{g}^\uparrow) &= -A^{(1)} e^{-i\phi} (B_{+-} S_{\tilde{b}} - B_{-+} C_{\tilde{b}}) (B_{+-} S_{\tilde{b}} - B_{-+} C_{\tilde{b}}) \frac{1 + \cos \theta}{2} \\
\mathcal{M}^{(2)}(b^\uparrow \bar{b}^\uparrow \rightarrow \tilde{g}^\uparrow \tilde{g}^\uparrow) &= A^{(2)} e^{-i\phi} (B_{--} S_{\tilde{b}} - B_{++} C_{\tilde{b}}) (B_{--} S_{\tilde{b}} - B_{++} C_{\tilde{b}}) \frac{1 + \cos \theta}{2} \\
\mathcal{M}(Z^\uparrow \rightarrow b^\downarrow \bar{b}^\downarrow) &= \frac{g_W}{\sqrt{2} \cos \theta_W} e^{i\phi} \left[(E + |\mathbf{p}|) g_L^b + (E - |\mathbf{p}|) g_R^b \right] \frac{1 - \cos \theta}{2} \delta^{ij} \\
\mathcal{M}^{(1)}(b^\downarrow \bar{b}^\downarrow \rightarrow \tilde{g}^\uparrow \tilde{g}^\uparrow) &= A^{(1)} e^{-i\phi} (B_{++} S_{\tilde{b}} - B_{--} C_{\tilde{b}}) (B_{++} S_{\tilde{b}} - B_{--} C_{\tilde{b}}) \frac{1 - \cos \theta}{2} \\
\mathcal{M}^{(2)}(b^\downarrow \bar{b}^\downarrow \rightarrow \tilde{g}^\uparrow \tilde{g}^\uparrow) &= -A^{(2)} e^{-i\phi} (B_{-+} S_{\tilde{b}} - B_{+-} C_{\tilde{b}}) (B_{-+} S_{\tilde{b}} - B_{+-} C_{\tilde{b}}) \frac{1 - \cos \theta}{2} \\
\mathcal{M}(Z^\uparrow \rightarrow b^\uparrow \bar{b}^\downarrow) &= -\frac{g_W m_b}{\sqrt{2} \cos \theta_W} (g_L^b + g_R^b) \frac{\sin \theta}{2} \delta^{ij} \\
\mathcal{M}^{(1)}(b^\uparrow \bar{b}^\downarrow \rightarrow \tilde{g}^\uparrow \tilde{g}^\uparrow) &= -A^{(1)} (B_{+-} S_{\tilde{b}} - B_{-+} C_{\tilde{b}}) (B_{++} S_{\tilde{b}} - B_{--} C_{\tilde{b}}) \frac{\sin \theta}{2} \\
\mathcal{M}^{(2)}(b^\uparrow \bar{b}^\downarrow \rightarrow \tilde{g}^\uparrow \tilde{g}^\uparrow) &= A^{(2)} (B_{--} S_{\tilde{b}} - B_{++} C_{\tilde{b}}) (B_{-+} S_{\tilde{b}} - B_{+-} C_{\tilde{b}}) \frac{\sin \theta}{2}
\end{aligned}$$

$$\begin{aligned}
\mathcal{M}(Z^\uparrow \rightarrow b^\downarrow \bar{b}^\uparrow) &= \frac{g_W m_b}{\sqrt{2} \cos \theta_W} e^{2i\phi} (g_L^b + g_R^b) \frac{\sin \theta}{2} \delta^{ij} \\
\mathcal{M}^{(1)}(b^\downarrow \bar{b}^\uparrow \rightarrow \tilde{g}^\uparrow \tilde{g}^\uparrow) &= A^{(1)} e^{-2i\phi} (B_{++} S_{\bar{b}} - B_{--} C_{\bar{b}}) (B_{+-} S_{\bar{b}} - B_{-+} C_{\bar{b}}) \frac{\sin \theta}{2} \\
\mathcal{M}^{(2)}(b^\downarrow \bar{b}^\uparrow \rightarrow \tilde{g}^\uparrow \tilde{g}^\uparrow) &= -A^{(2)} e^{-2i\phi} (B_{-+} S_{\bar{b}} - B_{+-} C_{\bar{b}}) (B_{--} S_{\bar{b}} - B_{++} C_{\bar{b}}) \frac{\sin \theta}{2}
\end{aligned}$$

\mathcal{M} matrix elements for $Z^\uparrow \rightarrow \tilde{b} \tilde{b} \rightarrow \tilde{g}^\uparrow \tilde{g}^\uparrow$:

$$\begin{aligned}
\mathcal{M}(Z^\uparrow \rightarrow \tilde{b} \tilde{b}) &= \frac{g_W}{\sqrt{2} \cos \theta_W} e^{i\phi} |\tilde{\mathbf{p}}| [g_L^b S_{\tilde{b}}^2 + g_R^b C_{\tilde{b}}^2] \sin \theta \\
\mathcal{M}^{(1)}(\tilde{b} \tilde{b} \rightarrow \tilde{g}^\uparrow \tilde{g}^\uparrow) &= \tilde{A}^{(1)} e^{-i\phi} |\tilde{\mathbf{p}}| (\tilde{B}_{--} S_{\tilde{b}}^2 + \tilde{B}_{++} C_{\tilde{b}}^2) \sin \theta \\
\mathcal{M}^{(2)}(\tilde{b} \tilde{b} \rightarrow \tilde{g}^\uparrow \tilde{g}^\uparrow) &= -\tilde{A}^{(2)} e^{-i\phi} |\tilde{\mathbf{p}}| (\tilde{B}_{++} S_{\tilde{b}}^2 + \tilde{B}_{--} C_{\tilde{b}}^2) \sin \theta
\end{aligned}$$

References

- [1] E. L. Berger, B. W. Harris, D. E. Kaplan, Z. Sullivan, T. M. P. Tait and C. E. M. Wagner, Phys. Rev. Lett. **86**, 4231 (2001) [arXiv:hep-ph/0012001].
- [2] G. C. Cho, Phys. Rev. Lett. **89**, 091801 (2002) [arXiv:hep-ph/0204348].
- [3] E. L. Berger and L. Clavelli, Phys. Lett. B **512**, 115 (2001) [arXiv:hep-ph/0105147].
- [4] L. J. Clavelli and L. R. Surguladze, Phys. Rev. Lett. **78**, 1632 (1997) [arXiv:hep-ph/9610493].
- [5] J. Cao, Z. Xiong and J. M. Yang, Phys. Rev. Lett. **88**, 111802 (2002) [arXiv:hep-ph/0111144].
- [6] L. Clavelli, Phys. Rev. D **46**, 2112 (1992).
- [7] C. W. Chiang, Z. Luo and J. L. Rosner, Phys. Rev. D **67**, 035008 (2003) [arXiv:hep-ph/0207235].
- [8] S. Berge and M. Klasen, Phys. Rev. D **66**, 115014 (2002) [arXiv:hep-ph/0208212].
- [9] P. Nelson and P. Osland, Phys. Lett. B **115**, 407 (1982).
- [10] B. Kileng and P. Osland, arXiv:hep-ph/9411248, Contributed to 9th International Workshop on High Energy Physics and Quantum Field Theory (NPI MSU 94), Moscow, Russia, 16–22 Sept. 1994.
- [11] B. A. Campbell, J. A. Scott and M. K. Sundaresan, Phys. Lett. B **126**, 376 (1983).
- [12] G. L. Kane and W. B. Rolnick, Nucl. Phys. B **217**, 117 (1983);

- [13] A. Djouadi and M. Drees, Phys. Rev. D **51**, 4997 (1995) [arXiv:hep-ph/9411314].
- [14] I. Terekhov and L. Clavelli, Phys. Lett. B **385**, 139 (1996) [arXiv:hep-ph/9603390].
- [15] L. M. Sehgal, Phys. Rev. **183**, 1511 (1969) [Erratum-ibid. D **4**, 1582 (1971)].
- [16] M. K. Gaillard and B. W. Lee, Phys. Rev. D **10**, 897 (1974).
- [17] M. E. Peskin and D. V. Schroeder, an Introduction to Quantum Field Theory, Perseus Books Publishing, L.L.C., 1995.
- [18] H. E. Haber and G. L. Kane, Phys. Rept. **117**, 75 (1985).
- [19] M. Drees, private communication. Certain expressions for B_0 and C_0 in the Appendix of Ref. [13] do not hold for all kinematic configurations. See other references (such as [20], [21]) for the complete expressions.
- [20] G. 't Hooft and M. J. Veltman, Nucl. Phys. B **153**, 365 (1979).
- [21] M. Drees, K. Hagiwara and A. Yamada, Phys. Rev. D **45**, 1725 (1992).
- [22] K. Cheung and W. Y. Keung, Phys. Rev. D **67**, 015005 (2003) [arXiv:hep-ph/0207219].
- [23] K. Cheung and W. Y. Keung, Phys. Rev. Lett. **89**, 221801 (2002) [arXiv:hep-ph/0205345].
- [24] R. Malhotra and D. A. Dicus, arXiv:hep-ph/0301070, to appear in Phys. Rev. D.
- [25] S. Baek, Phys. Lett. B **541**, 161 (2002) [arXiv:hep-ph/0205013].